Lecture 6 The Sun: From the Core to the Photosphere

Aims, learning outcomes, and overview

Aim: To introduce some of the physics associated with the Sun's interior and photosphere, including the energy release and transport processes, and to describe observational characteristics and modelling approaches of these regions.

Learning outcomes: At the end of this lecture, students are expected to:

- identify and describe qualitatively the different layers of the solar interior, from the core to the photosphere, including the basic physics;
- understand the energy production mechanisms in the Sun and the transport mechanisms of radiation and convection operating inside the Sun;
- describe and explain qualitatively the basic characteristics of sun spots and solar granulation;
- understand and describe qualitatively the basic techniques and results to date of helioseismology;
- understand and describe qualitatively mechanisms for magnetic buoyancy and dynamos, and evidence for their operation at the Sun;
- be able to describe recent insights into solar physics provided by solar neutrino measurements.

Overview: This lecture presents a survey of some basic physics of the Sun, focusing on the Sun's interior (from the core to the photosphere), recent developments in helioseismology and the Sun's rotation, ideas related to magnetic dynamos and buoyancy, and recent results involving solar neutrinos.

6.1 Interior structure of the Sun

The structure of the Sun may be divided into the solar atmosphere, i.e. that part of the Sun above the visible surface, or *photosphere*, and the solar interior. The solar interior is divided into the *core* region, the *radiative zone*, and the *convection zone*, in order of increasing distance from the centre. These divisions are based on the mechanisms of generation and transport of energy. Figure 6.1 illustrates the multiple layers of the nominal Sun, ranging from the core to the convective zone to the photosphere and then the various layers to the atmosphere. The photosphere is a thin layer in which the solar plasma goes from being almost completely opaque (the interior) to almost completely transparent (the atmosphere). Because we receive no

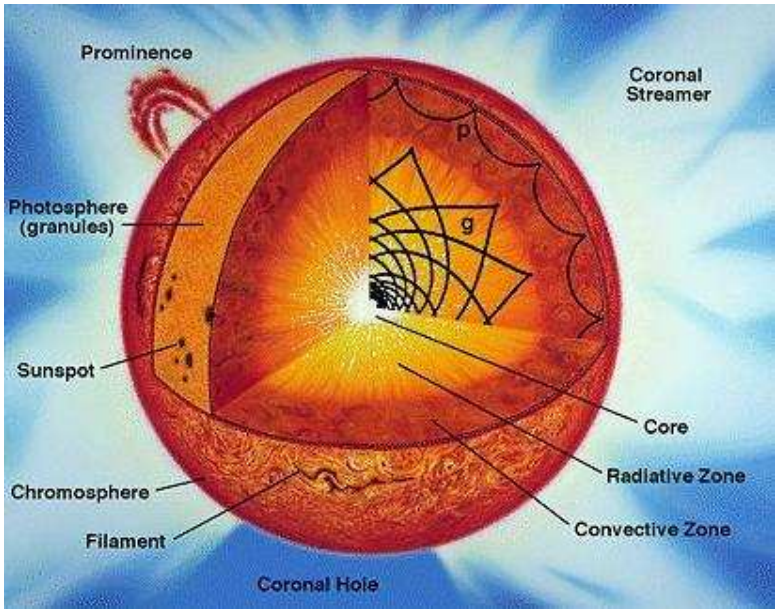

Figure 6.1: The multiple zones of the nominal Sun, from the solar interior to the corona. Acoustic wave patterns amenable to helioseismology investigations as well as magnetic loops are shown.

Quantity	Value
Radius	$R_\odot = 6.96 \times 10^8\,\mathrm{m}$
Distance from Earth	$1\,\mathrm{AU} = 1.50 \times 10^{11}\,\mathrm{m}$
Mass	$M_\odot = 1.99 \times 10^{30}\,\mathrm{kg}$
Acceleration at surface	$g_\odot = GM_\odot/R_\odot^2 = 274\,\mathrm{m\,s^{-1}}$
Luminosity	$L_\odot = 3.86 \times 10^{26}\,\mathrm{J\,s^{-1}}$
Photospheric temperature	5762 K
Solar age	4.60×10^9 years

Table 6.1: Some physical properties of the Sun.

light from below the photosphere, we have limited information about conditions in the solar interior. Our understanding is based on theoretical models, observations of solar neutrinos, and inferences from helioseismology. The solar atmosphere is amenable to direct observation in many wavelengths.

Some basic physical properties of the Sun are listed in Table 6.1.

6.1.1 Interior

6.1.1 Core and radiative zone

Fusion of hydrogen to helium is the primary energy production mechanism in the Sun, as is well known. This is made possible by the high internal temperature ($\approx 1.5 \times 10^7\,\mathrm{K}$) and density ($\eta \approx 1.6 \times 10^5\,\mathrm{kg\,m^{-3}}$). The principal set of reactions involves the conversion of Hydrogen into Helium, in three steps called the *proton-proton cycle*. A set of reactions involving heavier elements, the *CNO cycle* also occurs.

In detail the proton-proton cycle proceeds via the processes

$$^1H +^1 H \rightarrow {}^2H + e^+ + \nu_e + Q_1 \quad (6.1)$$

$$^2H +^1 H \rightarrow {}^3He + \gamma + Q_2 \quad (6.2)$$

$$^3He +^3 He \rightarrow^4 He +^1 H +^1 H + \gamma + Q_3 \ . \quad (6.3)$$

Or alternatively, in summary,

$$4p^+ \rightarrow^4 He^{2+} + 2e^+ + 2\nu_e + 2\gamma + Q_4 \ . \quad (6.4)$$

Thus energy is produced in the form of heat, gamma-rays, and electron neutrinos.

The simplest approach is to assume that fusion takes place in the innermost region of the core, with energy transported outwards from there by radiation. However, once suitable hydrogen ions (protons) are exhausted in the core (as a result of inadequate convection there), fusion is expected to take place in an annular ring that moves outwards. (Nuclear burning in the ring is typically considered to be relevant to stars moving off the Main Sequence towards the asymptotic Giant branch, something that the Sun is not expected to do for several billion years.) Of course, the initial cause for the Sun's central temperature exceeding the threshold for fusion to occur was due to conversion of gravitation potential energy into thermal energy as the solar nebula condensed and collapsed to form the Sun at its center. Outside the burning zone radiation propagates radially outwards, undergoing continual absorption and re-emission so that it is predicted to take in excess of a million years for radiation to travel from the core to the photosphere.

The core and radiative zones can be modelled with fluid equations (usually with the magnetic terms neglected) that include source terms for energy production (e.g., fusion) and loss (propagation) on their right hand sides. In these regions thermal pressure and radiation pressure balance the gravitational force.

Models for solar structure begin with the assumption of a hydrostatic balance between pressure and gravity [equation (2.37), with only pressure and gravity effects included]:

$$\frac{dP}{dr} = -\frac{Gm\eta}{r^2}, \quad (6.5)$$

where η is the local mass density, and m is the mass inside a sphere of radius r:

$$\frac{dm}{dr} = 4\pi r^2 \eta. \quad (6.6)$$

Spherical symmetry is assumed, and the effects of rotation, flows, and magnetic fields are ignored. Assuming an ideal gas we have $P = Nk_BT$ where N is the total number of particles per unit volume and T is the temperature. The mass density can be specified in terms of a mean atomic weight μ which is the average mass per particle in units of the proton mass m_H:

$$\eta = \mu m_{\rm H} N, \quad (6.7)$$

and hence

$$P = \frac{k_B}{\mu m_{\rm H}} \eta T. \quad (6.8)$$

Here N, P, T, and η are all functions of r. More accurate models will also have μ a function of r, due to burning of the nuclear fuel.

With the energy produced in the core, near the Sun's center, the energy and associated heat energy are expected to flow outward. This leads to a negative temperature gradient outwards. Eventually as η decreases convection becomes a more important energy transfer mechanism than radiation, leading to a change in behaviour and the start of the convection zone.

6.1.2 Convection zone

In the convective zone energy is transported primarily by convection, with hotter and less dense matter moving up (being buoyant) and cooler and denser material moving down. Different source terms are required in this region. Convection cells visible at and near the photosphere are directly observable manifestations of the convection zone. Perhaps even more importantly, though, convection is vital for understanding magnetic fields on the Sun. This is due to multiple effects, including evidence that the convection zone starts at the *tachocline*, the abrupt and narrow transition between the convection and radiative zones, the concentration of magnetic fields at the boundaries of convection zones (with resultant activity associated with *magnetic reconnection*.

Furthermore, there is strong evidence from multiple sources (sun spots, helioseismology, etc.) that the Sun rotates differentially from the base of the convection zone to the photosphere (faster at the poles, slower at the equator). This behaviour appears to start at the tachocline and is considered vital for the origin of magnetic fields on the Sun.

In the outer part of the Sun's interior, the convection zone, convective energy transport dominates over radiative transport. Convection is the bulk motion of a fluid in gas with a sufficient temperature gradient due to a simple instability described by Schwarzschild in 1906. Consider a parcel of gas at a radius r within the Sun, with temperature T, pressure P and density η, as shown in Figure 6.2. Assume the gas is transported to a radius $r + \Delta r$, where the ambient parameters are $T + \Delta T$, $P + \Delta P$, and $\eta + \Delta\eta$. The raised parcel of gas is assumed to have temperature $T+\delta T$, pressure $P+\delta P$ and density $\eta+\delta\eta$. If the gas is moved quickly enough so that the expansion of the parcel is adiabatic (i.e. $P \propto \eta^{\Gamma}$, where Γ is the adiabatic index), then

$$\frac{\delta\eta}{\eta} = \frac{1}{\Gamma}\frac{\Delta P}{P}, \tag{6.9}$$

where on the right hand side we have assumed that the lifting of the parcel is slow enough that the gas in the parcel remains in pressure balance with the ambient gas ($\delta P = \Delta P$). The parcel will continue to rise due to a buoyancy force if $\delta\eta < \Delta\eta$, or equivalently,

$$\frac{\delta\eta}{\eta} < \frac{\Delta\eta}{\eta}. \tag{6.10}$$

From the ideal gas relationship ($P \propto \eta T$),

$$\frac{\Delta\eta}{\eta} = \frac{\Delta P}{P} - \frac{\Delta T}{T}. \tag{6.11}$$

Using equations (6.9) and (6.11) the instability criterion (6.10) may be rewritten as

$$\frac{\Delta T}{T} < \frac{\Gamma - 1}{\Gamma}\frac{\Delta P}{P}, \tag{6.12}$$

or in the limit of small displacements,

$$\frac{dT}{dr} < \frac{\Gamma - 1}{\Gamma}\frac{T}{P}\frac{dP}{dr} = \left.\frac{dT}{dr}\right|_{\rm ad}. \tag{6.13}$$

This is the Schwarzschild stability condition. Both gradients are negative, so this equation says the parcel of gas will be unstable if the temperature gradient is sufficiently negative, i.e. sufficiently steep as a function of radius. Here the final form represents the temperature gradient in an ideal adiabatic gas.

In about the outer third of the solar atmosphere the temperature gradient is steeper than the adiabatic value (because the medium's opacity has increased due

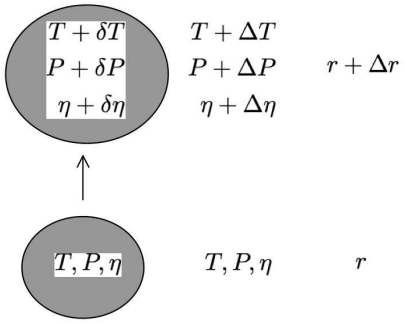

Figure 6.2: Set-up for derivation of the Schwarzschild criterion for the convective instability.

to the decreasing temperature), and convection occurs. The actual process of convection is a complex dynamic process in which warm gas rises, and then cools and falls again in convection cells. In a fluid of large viscosity convection cells are regular and stationary, but in the almost inviscid solar gas they become turbulent. There is no accepted, fully nonlinear theory for this turbulence, but an approximate "mixing length" theory can be developed and shown to yield reasonable agreement with observations. This theory is not described further here.

Three of the crucial manifestations of the convection zone are the granulation and supergranulation cells visible near the photosphere and the Sun's magnetic fields. These are discussed further below.

6.1.3 A solar model

Models for the Sun from the core to the photosphere can then be constructed, typically in the time-stationary, zero average velocity limit. Appropriate conditions include the Sun's total mass $m(R_\odot) = M_\odot$ and radiated energy flux (or luminosity) $L(R_\odot) = L_\odot$ and $\eta(R_\odot) = 0$. That is the density of material is assumed to be zero at the photosphere. Figure 6.3 illustrates a set of results.

6.2 Photosphere

Figure 6.4 illustrates the output of the Sun across the electromagnetic spectrum. (This figure is at the end of the document.) The Sun's atmosphere begins with the photosphere, which is seen in visible light. The radiative output of the Sun peaks in the visible, and the photospheric spectrum resembles a blackbody at a temperature of almost 6000 K. However, the Sun's spectrum in visible light is marked by a series of absorption lines called the the Fraunhofer lines. The photosphere is not uniformly bright but exhibits *limb darkening*, an effect which occurs because the temperature of the subphotosphere increases with depth. The light we see comes from a fixed optical depth along the line of sight, and as we move towards the limb, the oblique incidence of the line of sight with the solar surface means that the originating depth corresponds to a shallower radial depth into the Sun. Hence the light comes from cooler material near the limb, and the limb appears darker.

6.2.1 Sunspots

The photosphere is also marked by sunspots, which have been observed since Galileo. Sunspots are relatively cool regions compared with the surrounding photosphere, having $T \approx 4000$ K. They also have relatively strong magnetic fields at the surface (up to 0.4 Tesla or 4000 Gauss). It appears that the strong magnetic

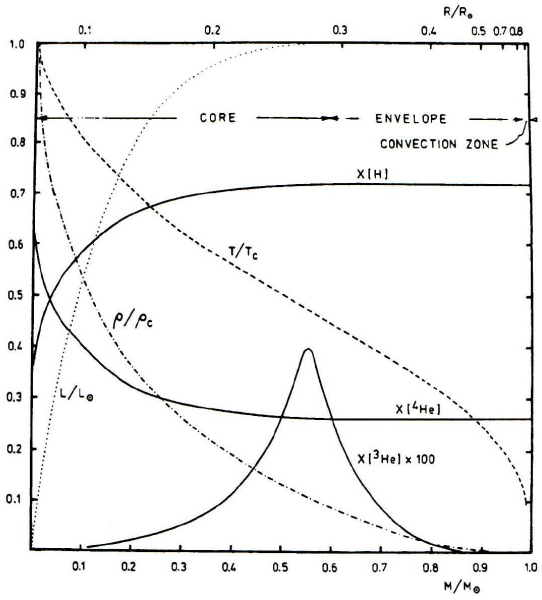

Figure 6.3: A standard solar model. The temperature T, mass density ρ, luminosity L, and fractional abundances by mass of H, ^{3}He and ^{4}He are plotted as functions of radius and mass. The central (scaling) factors are $T_c = 1.6 \times 10^7\,\mathrm{K}$ and $\rho_c = 1.6 \times 10^5\,\mathrm{kg\,m^{-3}}$. [From Bruzek and Durrant (1997).]

fields inhibit convection locally, and hence reduce the amount of energy reaching the surface. This can be understood simply in terms of magnetic tension forces, since convection of frozen-in magnetic field lines will attempt to bend the field lines against the straightening-out effect of the magnetic tension force (see Section 2).

Sunspots tend to occur in pairs because they are the result of the intersection of the photosphere with *magnetic flux tubes* (regions of strong magnetic field, with small field outside) that have emerged from below the photosphere (see Figure 6.7 below). Regions around magnetically connected sunspots are called *active regions* because they are centres of solar activity, and in particular the sites of occurrence of *solar flares*.

Sunspots reveal the Sun's rotation. The Sun is a fluid, and does not rotate as a rigid body – the Sun exhibits *differential rotation*, with the rotation rate being fastest at the equator. Figure 6.5 shows a number of measurements of solar differential rotation, based on different markers of the fluid motion. There is no generally accepted theory for the observed differential rotation, and in fact it is at odds with simple theory, which predicts that, because of a circulation set up by the rotation-induced oblateness of the solar sphere, the pole should rotate faster than the equator. More than a century ago, Carrington determined an average rotation rate for sunspots of about 27.28 days, as observed from Earth (the *synodic* rotation rate – the corresponding rotation rate with respect to the distant stars, the *sidereal* rate, is 25.38 days).

6.2.2 Granulation and supergranulation cells

Also visible on the photosphere is a changing (on the order of minutes) cellular pattern called *granulation*, illustrated in Figure 6.6. The bright granules are rising hot gas, and the dark lanes between them are cooler, falling gas (the velocities

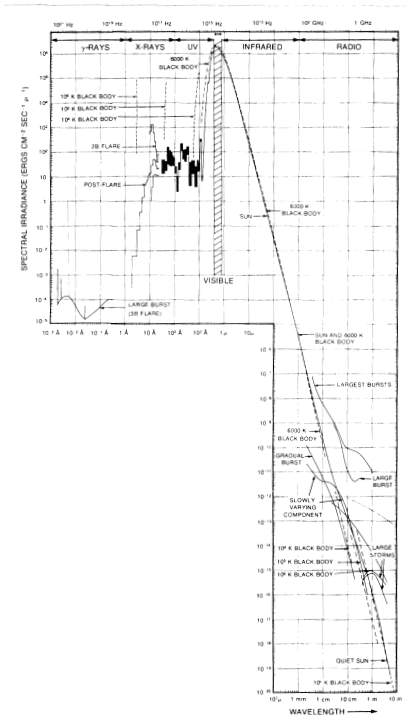

Figure 6.4: The spectrum of the Sun. [From Golub and Pasachoff (1997).]

are around $1\,\mathrm{km\,s^{-1}}$). Granulation is direct evidence for the turbulent convection occurring below the photosphere. Granular diameters appear to follow a continuous distribution, although they are usually not larger than about $2''$ ($\approx 1.4 \times 10^6\,\mathrm{m}$).

There is also a larger scale organisation into *supergranules* with typical size $3 \times 10^7\,\mathrm{m}$, which is visible in doppler velocity measurements of photospheric flows. The borders between supergranules correspond with the sites of emission in certain spectral lines (notably CaII) formed slightly higher in the solar atmosphere: the *chromospheric network*. The connection is provided by the magnetic field, which tends to become concentrated in the intra-network lanes by the supergranular flow pattern. For reasons that are not well understood, additional heating occurs in the chromosphere at sites of enhanced magnetic field, as discussed in the next lecture.

6.3 Magnetic dynamos, buoyancy, and photospheric fields

The magnetic field at the photosphere may be inferred from its effect on spectral lines in the low solar atmosphere – the Zeeman effect. Magnetographs are used to infer the line of sight magnetic field, and vector magnetographs, or Stokes Polarimeters may be used to infer the transverse magnetic field.

Flux emerges in sunspot regions because it is buoyant, as argued by Parker and understood very simply in terms of pressure balance. As shown in Lectures 2 and 5, the Lorentz force may be interpreted as consisting of a magnetic tension and the gradient of a magnetic pressure, $B^2/(2\mu_0)$, while normal momentum balance involves the ram pressure, thermal pressure, and transverse magnetic field. For a stable and static magnetic flux tube there must be a balance normal to the flux

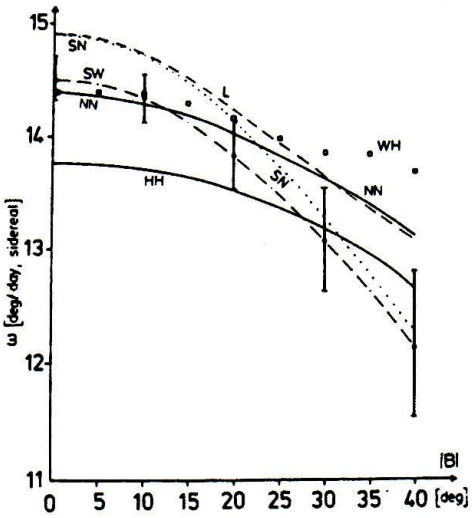

Figure 6.5: Differential rotation. Rotation rates for sunspots (NN), photospheric plasma (HH), chromospheric plasma in Hα (L), photospheric magnetic field (WH), coronal plasma (SN), and features in Ca II (SW). [From Bruzek and Durrant (1997).]

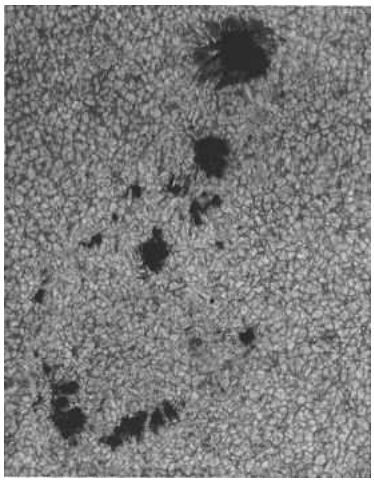

Figure 6.6: The photosphere in white light, showing small sunspots and granules. [From Stix (1989).]

tube's surface of sum of the thermal fluid pressure and the magnetic pressure inside the tube, and the thermal pressure outside the tube, neglecting the magnetic field outside the tube and the ram pressure terms. In other words,

$$P_{ext} = P_{int} + B_t^2/(2\mu_0), \tag{6.14}$$

where P_{int} and P_{ext} denote the internal and external gas pressures, respectively, and B_t is the magnetic field in the flux tube. Assuming the temperatures inside and outside the flux tube are equal, and that the fluid obeys the ideal gas equation ($P \propto \eta T$), we have that

$$\frac{\eta_{ext} - \eta_{int}}{\eta_{ext}} = \frac{B^2}{2\mu_0 P_e}. \tag{6.15}$$

Hence $\eta_{int} < \eta_{ext}$, and the flux tube is buoyant.

Figure 6.7) illustrates this process, as well as one effect counteracting it, that of magnetic tension forces. Convection can also counteract this buoyancy process, especially when the field is weak and the magnetic pressure is small compared with the thermal and ram pressure terms. The basic point, though, is that the magnetic fields tend to be buoyant.

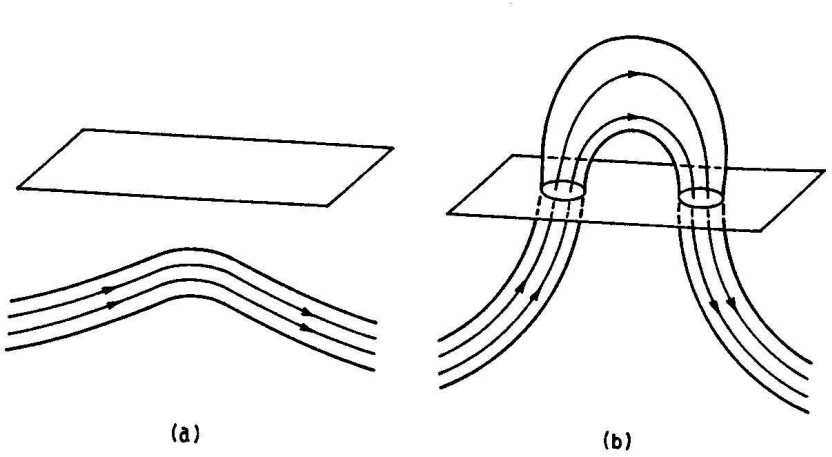

Figure 6.7: A flux tube beneath the photosphere (a). In (b), the flux tube has emerged, and the regions of intersection with the photosphere may form sunspots. [From Choudhuri (1998).]

Figure 6.7 illustrates, then, why magnetic field lines tend to rise up, form pairs of sun spots, and form magnetic loops in the solar atmosphere. In the photosphere and higher the medium becomes increasingly ionized and the ratio of the magnetic energy density to the thermal energy density becomes large, so that the magnetic field now quantitatively affects the motion of the plasma.

Convection, together with the Sun's rotation, is thought to be responsible for the generation of intense localised magnetic fields observed at the surface of the Sun, and hence for *solar activity*, which is a variety of dynamic phenomena associated with magnetic fields. The *solar dynamo* (the mechanism generating the fields) was originally thought by theorists to reside in the convection zone, but the results of helioseismology are inconsistent with the requirements of the models, and the dynamo is now believed to operate at the base of the convection zone, the *tachocline*, where there are strong radial gradients in the rotation rate. Values for the depth

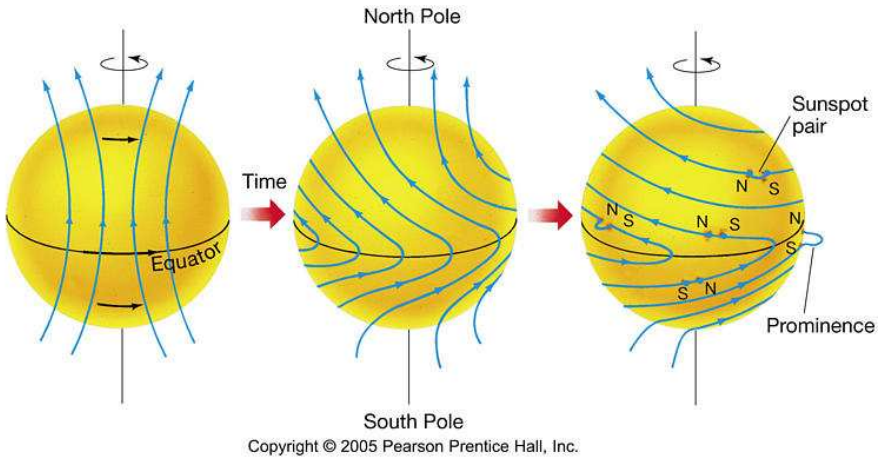

Figure 6.8: Generation of toroidal magnetic field from a poloidal field due to differential rotation. [From Pearson Prentice Hall 2005.]

of the convection zone, derived from helioseismology (§ 6.2), are typically close to $0.7R_\odot$.

Magnetic dynamo theory involves the magnetic induction equation (2.35 in Lecture 2)

$$\frac{\partial \mathbf{B}}{\partial t} = \boldsymbol{\nabla} \times (\mathbf{U} \times \mathbf{B}) + \frac{1}{\mu_0 \sigma} \nabla^2 \mathbf{B} \; , \tag{6.16}$$

an equation of motion for the magnetized fluid

$$\eta \left[\frac{\partial \mathbf{U}}{\partial t} + (\mathbf{U} \cdot \boldsymbol{\nabla}) \mathbf{U} \right] = -\nabla p + \mathbf{J} \times \mathbf{B} + \eta \mathbf{g} \, . \tag{6.17}$$

an Ohm's Law, plus whatever other equations are required to form a closed system. Rotation and convection, including the effects of turbulence, turn out to be vital. In Eq. 6.16 the diffusion term is typically a loss term, so that magnetic amplification involves the curl of $\mathbf{U} \times \mathbf{B}$ term.

A dynamic magnetic dynamo involves flow and magnetic fields that can self-consistently maintain and/or amplify a magnetic field. This is often discussed in terms of an α effect and an Ω effect. The Ω effect involves the generation of a toroidal magnetic field from a poloidal field in the presence of differential rotation for frozen-in fields. This is illustrated in Figure 6.8: the differential rotation pulls the initially poloidal field into the poloidal direction and wraps it around, generating a poloidal field.

The re-generation of poloidal field from a toroidal field, the so-called α effect is more complicated. It involves magnetic turbulence that contributes a non-zero time-averaged current in the Ohm's Law, with

$$< \mathbf{J} >= \sigma(< \mathbf{E} > + < \mathbf{u} > \times < \mathbf{B} > + < \mathbf{u}' \times \mathbf{B}' >) \; . \tag{6.18}$$

When

$$< \mathbf{u}' \times \mathbf{B}' >= \alpha < \mathbf{B} > \tag{6.19}$$

then there is a current along the average magnetic field direction $< \mathbf{B} >$ and so a magnetic field is generated transverse to the average magnetic field. This allows a poloidal magnetic field to be generated from a toroidal field.

Thus differential rotation and turbulence appear to be required to form a persisting magnetic dynamo. Dynamo theory remains a very active area of research.

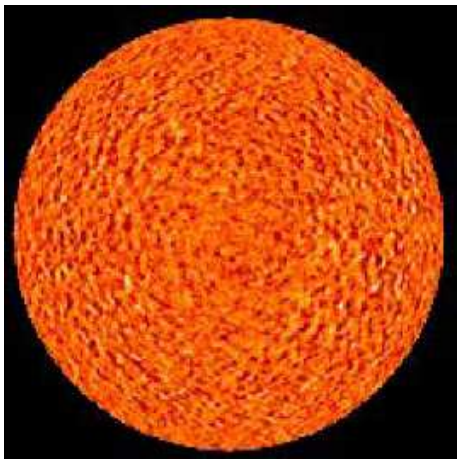

Figure 6.9: Snapshot of the Sun, showing the convective cells subject to helioseismic oscillations.

6.4 Helioseismology

Helioseismology is an exciting area of solar physics that has developed in the last few decades, focusing on wave propagation in the solar interior. The subject derives its name from the analogy with the study of wave propagation in the Earth's interior (seismology). Helioseismic observations have allowed accurate measurement of the depth of the convection zone, as well as inference of the Sun's internal rotation profile and internal temperature – measurements that were previously thought to be impossible to make.

Since 1960 it has been known that the surface of the Sun oscillates, with about half of the Sun (at any time) occupied by oscillatory patches (period $\approx 5\,\mathrm{min}$, amplitude $\approx 1\,\mathrm{km\,s^{-1}}$). The oscillations last about six or seven periods, and areas as large as $30,000\,\mathrm{km}$ often oscillate in phase. Figure 6.9 illustrates these oscillations.

At first this was thought to be a local phenomenon, but now it is known that the oscillations are a superposition of global acoustic modes of the Sun. A theory accounting for the five-minute oscillations as standing acoustic waves, trapped in the convection zone was presented by Ulrich and also Leibacher and Stein around 1970. The observational confirmation of the theory was made by Deubner in 1975. Figure 6.10 shows one observational indication of the global nature of the modes, namely distinct peaks in the power spectrum of unresolved observations.

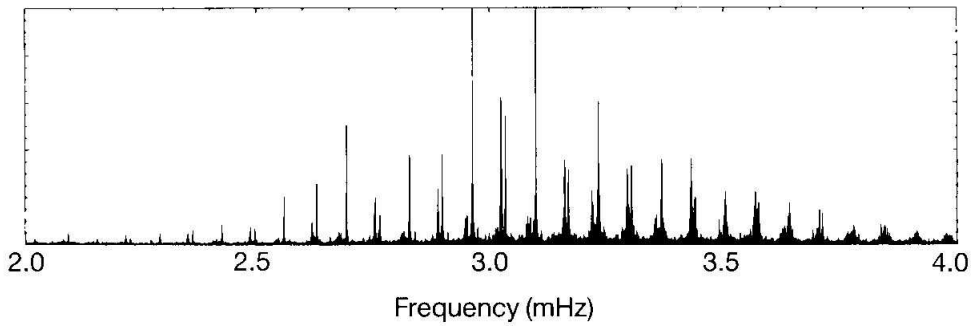

Figure 6.10: Power spectrum of global solar oscillations, from 3 months of integrated-light observations. [From Phillips (1992).]

The theoretical treatment of solar oscillations begins with the linearisation of the equation of motion and the continuity equation for perturbations of a gravitationally stratified, adiabatic fluid [see Stix (1989) for a more complete description]. Rotation and the influence of a magnetic field are neglected in the basic theory. Fluid perturbations are expressed as expansions in spherical harmonics, so that, for example, the radial component of the fluid displacement is written

$$\xi(\mathbf{r}, t) = \exp(i\omega t)\xi_r(r)Y_l^m(\theta, \phi). \tag{6.20}$$

For each *degree* l, there are many possible eigenfunctions ξ_r, which are labelled with an integer n, called the order of the mode. The value of n determines the number of radial nodes in the eigenfunction. The degree l and *azimuthal order* m define the number of node circles on the sphere and the number of node circles passing through the poles, as shown in Figure 6.11. On a stationary Sun there are no poles, and so the eigenfrequencies must be independent of m, a degeneracy that is analogous to that in the quantum mechanical description of the energy levels of the Hydrogen atom. Rotation introduces a preferred axis and removes this degeneracy, splitting the eigenfrequencies.

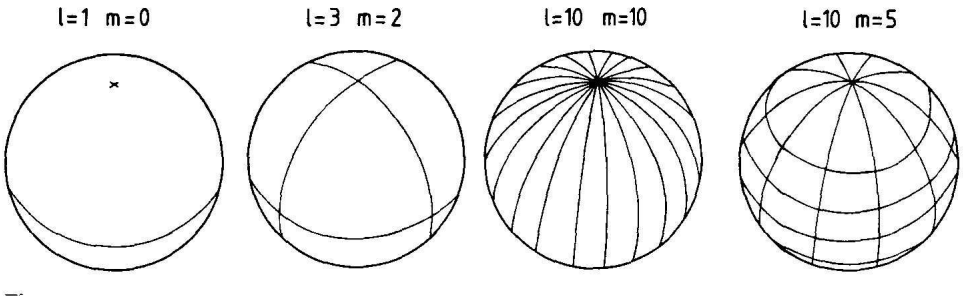

Figure 6.11: Node circles of spherical harmonics. [From Stix (1989).]

The restoring forces for solar oscillations are either pressure or buoyancy (gravity). For the 5-minute oscillations pressure is most important, and so the observed oscillations are called *p-modes*. The modes are thought to be continually excited by turbulence in the convection zone. The modes which have gravity as the restoring force are called *g-modes*. Calculation suggests that these modes are predominantly trapped in the solar interior, and are not detectable at the solar surface. There is considerable interest in the possibility of detecting g modes and using them for seismology, because they probe the deep interior of the Sun, but to date there has been no generally accepted detection. There are also surface waves, called *f-modes*.

There are two observational approaches in helioseismology. Doppler measurements with no spatial resolution may be used to determine the signal of low-l modes. High-l modes require spatial resolution. The best helioseismic measurements to date have come from the Michelson Doppler Interferometer (MDI) instrument on the Solar and Heliospheric Observer (SOHO) spacecraft.

Because the mode frequencies depend on the internal sound speed of the Sun, it is possible to take the observed spectrum of frequencies and solve the inverse problem to obtain the sound speed as a function of radius. Figure 6.12 shows an example, together with the sound speed predicted by a solar model. The curves agree almost to within the thickness of the line (although in fact they disagree more than the estimated errors). The base of the convection zone is detectable as a change in curvature at about $0.7R_\odot$. The inversions are quite reliable, and confirm the structure predicted by standard stellar evolution theory.

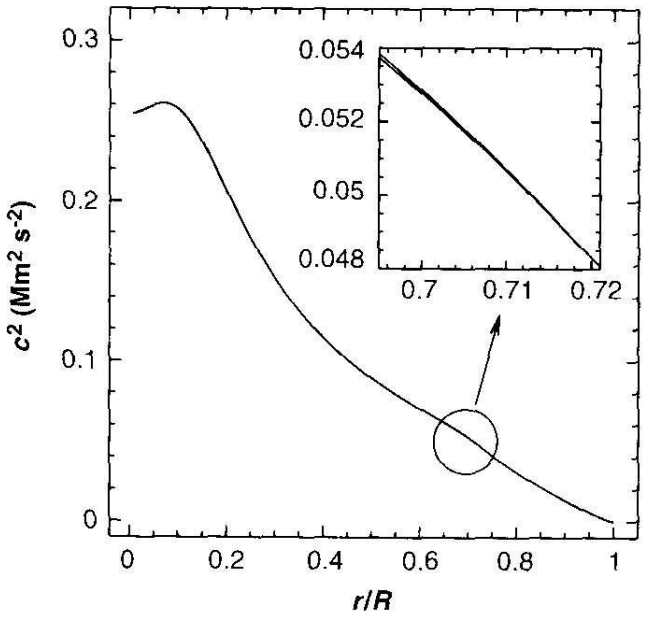

Figure 6.12: The internal sound speed of the Sun, inferred from helioseismology data, together with sound speed predicted by a standard solar model. The agreement is within the thickness of the lines in the larger picture. [From Deubner & Gough (1984).]

The degree of splitting of the p-modes depends on the internal rotation of the Sun. It is also possible to take the observed splittings and infer how the rotation rate varies inside the Sun. Figure 6.13 shows an example. The main features of the inferred rotation profile are that differential rotation ends at the base of the convection zone, i.e. the radiative zone and core rotate (almost) rigidly, and that the rotation in the convection zone is almost constant along radial lines. Hydrodynamic models of rotation have considerable difficulty accounting for these basic features.

Finally we mention a recent development, local helioseismology. By examining the correlations of p-mode oscillations on the surface of the Sun observed at high resolution, it is possible to infer the local variation of sound speed with depth. It is also possible to infer the magnetic field as a function of position below sunspots using "sunquakes" and other localized sources of waves.

6.5 Solar neutrino observations and arguments for fusion

Until early in the 20th century, it was believed that the Sun was continually collapsing, releasing gravitational potential energy in the process, and this process was thought to power the Sun. The total gravitational potential energy of the Sun is about

$$\Omega_\odot = -GM_\odot^2/R_\odot \approx -4 \times 10^{41}\,\mathrm{J}, \tag{6.21}$$

and the present luminosity of the Sun is $L_\odot \approx 3.9 \times 10^{26}\,\mathrm{W}$. Assuming continual conversion of gravitational potential energy to solar output, at its present luminosity the Sun would last about the *Kelvin-Helmholtz time*,

$$\tau_{\mathrm{KH}} = \Omega_\odot/L_\odot \approx 10^{15}\,\mathrm{s} \approx 3 \times 10^7\,\mathrm{y}. \tag{6.22}$$

Hence until the early 1900s it was believed that the Sun and the Earth are a few tens of million years old. However, geological evidence pointed to a much older Earth

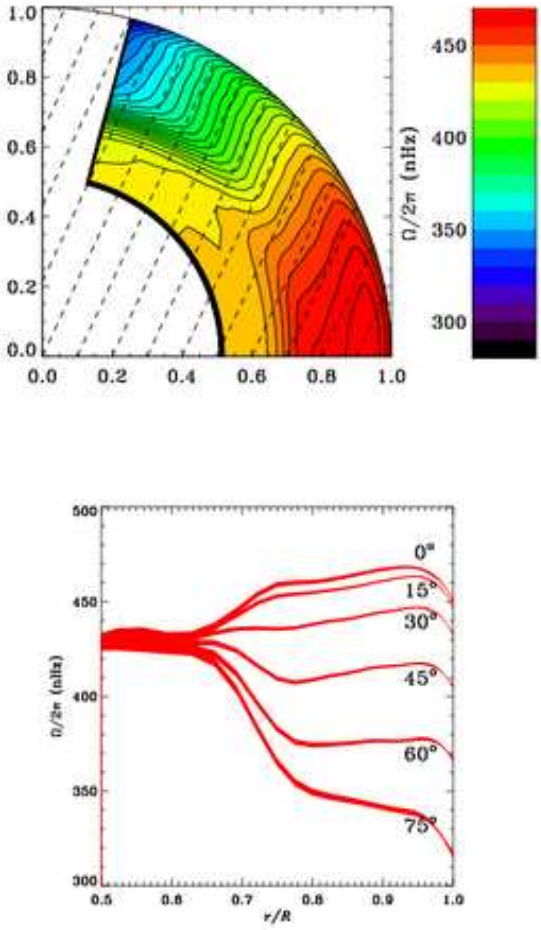

Figure 6.13: (Left) The internal rotation profile of the Sun, inferred from GONG helioseismology. The units are nano-Hz. (Right) Cuts at different heliolatitudes for the rotation rate as a function of radial distance, also from GONG.

(the currently accepted age for the Sun and the Earth is about 4.6×10^9 y). In 1929 Eddington was among the first to argue that the Sun must be fueled by a subatomic source of energy. A detailed theoretical explanation of the nuclear processes occurring in the Sun's core was provided by Hans Bethe in 1939, although because the temperature of the interior was thought to be higher than the accepted value today, Bethe favoured the CNO cycle as the dominant process. The final confirmation of the fusion hypothesis was the observational detection of solar neutrinos, which are produced by the nuclear reactions in the Sun's core.

Neutrinos are fundamental particles that have no charge and have a very small (or zero) mass. They interact only via the weak force, and the cross section for interaction is very small, so matter is effectively transparent to neutrinos. An enormous number of neutrinos are produced in the core of the Sun – of order $10^{38}\,\mathrm{s}^{-1}$. The longest-running experiment to detect solar neutrinos was started by Ray Davies in 1967. The experiment is 1.5 km underground in the Homestake mine in South Dakota, and consists of a tank containing 380,000 litres of cleaning fluid. The fluid contains a large number of Chlorine atoms. About every two days, one Chlorine atom undergoes the reaction

$$\nu_e + {}^{37}\mathrm{Cl} \rightarrow e^- + {}^{37}\mathrm{Ar}. \tag{6.23}$$

The ^{37}Ar atom produced is subsequently detected by its decay back to ^{37}Cl.

After the Homestake experiment had been run for some time, it was realised that too few neutrinos were being observed (by about a factor of three), compared with the predictions from standard solar models. The observed deficit was known as the *solar neutrino problem*. Figure 6.14 illustrates the results from the Homestake experiment and the theoretical predictions for that experiment (far left, labelled 'Cl'). Subsequent solar neutrino experiments confirmed the deficit and its approximate value. The Japanese Kamiokande experiment (and the later Super-Kamiokande) used the scattering of neutrinos on electrons via detection of the Cerenkov radiation produced by the electrons. These experiments gave information about the direction of flight of the neutrinos, and confirmed that the observed neutrinos come from the Sun.

The solar neutrino problem indicated a deficiency in either the understanding of the Sun (and hence of stellar modelling), or in the standard model for neutrinos. However, the consistency of solar models with heliospheric results suggested that the problem was with the neutrino. According to the standard particle physics model, there are three varieties (flavours) of neutrino: the electron, tau, and mu neutrino. Solar neutrinos are generated as electron neutrinos, and only electron neutrinos are detected by the Homestake and Kamiokande experiments. However, if the neutrino changes its flavour enroute to Earth (*oscillate*), a deficit in neutrinos would be observed. Further, if a neutrino is equally likely to arrive at Earth as any flavour, i.e. if there is *strong mixing*, then the detected flux would be reduced by a factor of three, reconciling theory and observations. For oscillations to occur, neutrinos require a finite rest mass, but the standard particle physics model says that the neutrino rest mass is zero. Recently, experimental evidence for neutrino oscillations was obtained. The Sudbury Neutrino Observatory (SNO) has simultaneously run an experiment sensitive to only electron neutrinos and an experiment sensitive to all three neutrino flavours (Ahmad et al. 2002). The inferred flux for the second experiment was three times that of the first experiment, consistent with strong mixing. The total flux of neutrinos was found to be consistent with the standard solar model, so that the neutrino problem finally appears to have been resolved. In 2002 the Nobel Prize in Physics was partly awarded to Ray Davis and to Masatoshi Koshiba, the leader of the original Kamiokande experiment.

Figure 6.14: Solar neutrino flux measurements from a variety of experiments and theoretical predictions. On the far left are the original measurements from the Homestake experiment, and the theoretical predictions for that experiment. Results for the Sudbury Neutrino Observatory (SNO) are shown at the far right. These results appear to solve the solar neutrino problem. [From John Bahcall's web pages: http://www.sns.ias.edu/∼jnb/.]

References

Ahmad, Q.R., et al. 2002, *Phys. Rev. Lett.*, **89**, 011301

Bahcall, J.N. 1989, *Neutrino Astrophysics*, Cambridge University Press, Cambridge

Bowers, R.L. and Deeming, T. 1984, *Astrophysics I: Stars*, Jones and Bartlett, Boston

Bruzek, A. and Durrant, C.J. (eds.) 1977, *Illustrated Glossary for Solar and Solar-terrestrial Physics*, D. Reidel, Dordrecht

Choudhuri, A.R. 1998, *The Physics of Fluids and Plasma: An Introduction for Astrophysicists*, Cambridge University Press, Cambridge

Cox, A.N., Livingston, W.C. and Matthews, M.S. (eds.) 1991, *Solar Interior and Atmosphere*, University of Arizona Press, Tucson

Deubner, F.L. and Gough, D. 1984, Annual Reviews of Astronomy and Astrophysics **32**, 593

Gibson, E.G. 1973, *The Quiet Sun*, NASA SP-303

Golub, L. and Pasachoff, J.M. 1997, *The Solar Corona*, Cambridge University Press, Cambridge

Phillips, K. 1992, *Guide to the Sun*, Cambridge University Press, Cambridge

Stix, M. 1989, *The Sun: An Introduction*, Springer-Verlag, Berlin